Rare Metal Materials and Engineering
Volume 48, Issue 10, October 2019
Available online at www.rmme.ac.cn

Science Press

Cite this article as: Rare Metal Materials and Engineering, 2019, 48(10): 3124-3129.

ARTICLE

Effect of Pressure on the Structural, Electronic, and Physical Properties of $Mg_3Zn_3Y_2$: a First-Principles Calculations

Gao Yan[1,2], Mao Pingli[1], Liu Zheng[1], Wang Feng[1], Wang Zhi[1]

[1] Shenyang University of Technology, Shenyang 110870, China; [2] Shenyang Normal University, Shenyang 110034, China

Abstract: The first-principles calculations were performed to investigate the structural, elastic and electronic properties of typical face-centered cubic precipitate of $Mg_3Zn_3Y_2$ under high pressure based on density functional theory (DFT). The elastic constants of $Mg_3Zn_3Y_2$ were calculated and analyzed. The bulk modulus (*B*), shear modulus (*G*), Young's modulus (*E*), Poisson's ratio (*v*), anisotropy index (*A*), melting points and hardness were further calculated based on the elastic constants. The calculation results show that the optimized lattice constants of $Mg_3Zn_3Y_2$ at 0 GPa are similar to those of other calculated and experimental results. The physical properties of $Mg_3Zn_3Y_2$ change positively with the increase of pressure. In addition, the anisotropy index (*A*) of $Mg_3Zn_3Y_2$ increases as the pressure increases. The electronic density of states (DOS) of $Mg_3Zn_3Y_2$ phase was analyzed, and it is revealed that the structural stability of the $Mg_3Zn_3Y_2$ phase decreases as the pressure increases.

Key words: first principles calculation; magnesium alloy; elastic properties; electronic structure

Magnesium alloys are increasingly applied ranging from microelectronics to automobile, aviation, electronic communication, medicine and aerospace industries owing to their low density, good stiffness and the highest strength-to-weight ratio[1-3]. However, their further development were still limited due to their relatively poor ductility[4]. Therefore, many efforts have been devoted to developing new magnesium alloys with better ductility. Resent research results indicating that an effective solution to enhance the strength of magnesium alloys was to add rare earth elements in the alloys[5]. Mg-Zn-Y series ternary alloys has attracted intensive attention due to its excellent mechanical properties and unique crystal structure[6]. Up to now, many researchers have reported the phase properties and thermal stability of Mg-Zn-Y alloys, especially the binary phases, such as $MgZn_2$, Mg_2Zn, MgY and Mg_2Y, whereas only little attention has been paid to ternary equilibrium phases. Three kinds of ternary equilibrium phases have been found forming in Mg-Zn-Y alloys system, which are W-$Mg_3Zn_3Y_2$, I-Mg_3Zn_6Y and X-$Mg_{12}ZnY$ phases[7,8]. In later researches X-$Mg_{12}ZnY$ was proved to have a long period stacking ordered structure (LPSO) and it was replaced by a name of 18R. Tang et al[7] investigated the structural, elastic and electronic properties of $Mg_3Zn_3Y_2$ phase in Mg-Zn-Y system. It was found that the highest structural stability of W-$Mg_3Zn_3Y_2$ phase was attributed to the increase in the bonding electron numbers below the Fermi level. Ma et al[9] studied the crystal structures, enthalpies of formation and electronic structures of 18R and W-$Mg_3Zn_3Y_2$ phase in Mg-Zn-Y system. It was found that W-$Mg_3Zn_3Y_2$ phase was more stable than 18R phase. The thermodynamic stabilities and electronic characteristics of 18R and 14H in Mg-Zn-Y alloys have been studied by Ma et al[10] and it was found that 14H was more stable than 18R.

Although much effort has been made to investigate the physical properties of the ternary equilibrium phases in Mg-Zn-Y systems, most of the previous work was carried out under zero pressure. It was well known that pressure has a great influence on the mechanical properties of the material[11]. Under high pressure, the structure and properties of the material will exhibit different performances with 0 GPa. Under pressure, the dislocation density of the material will decrease and the strength will increase. If the pressure is high

Received date: October 25, 2018
Foundation item: National Natural Science Foundation of China (51571145); Shenyang Science and Technology Plan (17-9-6-00)
Corresponding author: Mao Pingli, Ph. D., Professor, School of Materials Science and Engineering, Shenyang University of Technology, Shenyang 110870, P. R. China, Tel: 0086-24-25497131, E-mail: maopl@sut.edu.cn

enough, the dislocations of the material can even disappear, and the strength of the material will increase by several orders of magnitude. Peivaste et al[12] investigated the mechanical properties of three different SiC polytypes under high pressure. Calculations showed that the three SiC structures were mechanically stable with high hardness properties. Guo et al[13] investigated the structural, mechanical and electronic properties of thorium dichalcogenides under high pressure. It was found that a pressure-induced semiconductor to metal transitions of three compounds will occur. Therefore, the study of the influence of pressure on material properties will be of great significance for promoting material development.

In the present work, the first-principles calculations were used as a theoretical method to study the crystal structural stability, electronic structure and elastic properties of W-$Mg_3Zn_3Y_2$ phase under the pressure ranging from 0 GPa to 100 GPa with a step of 10 GPa. The variation of lattice parameters, elastic properties and electronic structure under high pressures were analyzed.

1 Computational Methods

The calculations were performed by the density functional theory (DFT)[14], using the CASTEP code[14,15]. The plane wave pseudo-potentials method was used and the exchange-correlation terms in the electron-electron interaction was treated with the Perdew-Bruke-Ernzerhof (PBE) version of generalized gradient approximation (GGA)[16-18]. The cut-off energy of plane wave was set to 380 eV. The k-points of Monkhost-Pack scheme was set to 6×6×6 for structural optimization and self-consistent energy calculations. The total energy convergence value was 5.0×10^{-5} eV/atom, tolerance displacement was within 5.0×10^{-5} nm, the force on all atoms was less than 0.01 eV/nm and stress deviation was within 0.02 GPa.

2 Results and Discussion

2.1 Crystal structure and stability

W-$Mg_3Zn_3Y_2$ phase is a face-centered-cubic structure with the space group of Fm-3m and the Pearson symbol of cF16. There are 16 atoms in the primitive unit cell of $Mg_3Zn_3Y_2$, where four Mg atoms occupy the 4b site (0.5, 0.5, 0.5), eight Mg atoms occupy the 8c site (0.25, 0.25, 0.25), eight Zn atoms occupy the 8c site (0.25, 0.25, 0.25) and four Y atoms occupy the 4a site (0, 0, 0). The structure of $Mg_3Zn_3Y_2$ is shown in Fig.1. The optimized lattice parameters of W-$Mg_3Zn_3Y_2$ phase at 0 GP are shown in Table 1. For comparison the experimental and theoretical values obtained by other authors are followed in Table 1[7,9]. As can be seen that the calculated values in the present paper are in good agreement with experimental data and the calculated results by other authors, implying that the calculation parameters in the present paper are reasonable.

The normalized lattice parameters a/a_0 and V/V_0 in the range from 0 GPa to 100 GPa are shown in Fig.2, where a_0 and V_0 are the parameters at 0 GPa. It can be seen that both

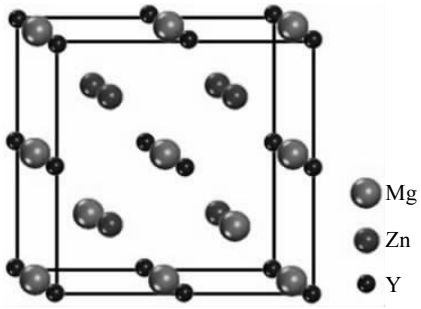

Fig.1 Crystal structure of $Mg_3Zn_3Y_2$ compound

Table 1 Lattice constants (a_0, V_0) and ρ of $Mg_3Zn_3Y_2$ at zero pressure

Parameter	$a_0/\times10^{-1}$ nm	$V_0/\times10^{-3}$ nm	ρ/g·cm^{-3}
Present	6.981	340.17	4.363
Cal.[7]	6.924	334.86	-
Cal.[9]	6.974	-	-
Exp.[7,9]	6.848	321.14	-

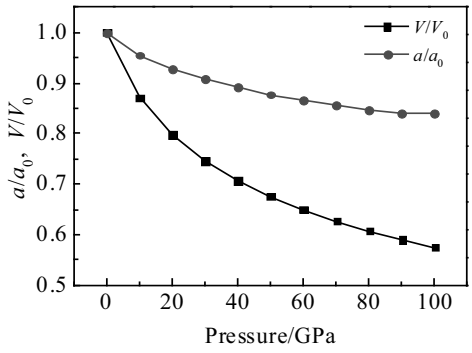

Fig.2 Normalized lattice parameter a/a_0 and the normalized volume V/V_0 of $Mg_3Zn_3Y_2$ as a function of pressure

a/a_0 and V/V_0 decrease gradually as the pressure increases. These variations indicate that the atoms in the interlayer become closer, and their interactions become stronger. When the external pressure reaches 100 GPa, the a-axis is shortened by about 16.1% and the volume is reduced by about 42.5%. By fitting these ratios of a/a_0 and V/V_0, the following quadratic functions can be obtained, where the unit of pressure is GPa.

$$a/a_0 = 0.99054 - 0.00314P + 1.64815\times10^{-5}P^2 \quad (1)$$

$$V/V_0 = 0.96687 - 0.00817P + 4.42972\times10^{-5}P^2 \quad (2)$$

2.2 Elastic properties

The ability of a material to resist external forces is mainly characterized by elastic properties. The elastic properties of a material, such as bulk modulus B, shear modulus G, Young's modulus E, Poisson's ratio v and anisotropy A, play an important role in understanding the mechanical, dynamic and thermodynamic behaviors of materials[19,20]. W-$Mg_3Zn_3Y_2$ phase

has a cubic crystal structure, which has three independent elastic constants C_{11}, C_{12} and C_{44}. The stability criteria of the cubic crystals are listed below[21]: $(C_{11}+2C_{12})>0$, $C_{11}-C_{12}>0$, $C_{11}>0$, $C_{44}>0$. The calculated elastic constants of $Mg_3Zn_3Y_2$ at 0 GPa are shown in Table 2. It can be seen that the results of the present paper are consistent with Ref.[7]. In addition, it can be inferred that $Mg_3Zn_3Y_2$ is a stable phase because it fully satisfies the conditions for mechanical stability.

To understand the mechanism of mechanical stability, the influence of external pressures on the elastic constants (C_{ij}) of W-$Mg_3Zn_3Y_2$ phase was investigated and the results are shown in Fig.3. It can be seen that all elastic constants increase linearly with increasing pressure and they still satisfy the mechanical stability conditions. The change in C_{11} is more sensitive than in C_{12} as pressure increases because of the differences in compressibility in different directions. Further, it can be found that the $Mg_3Zn_3Y_2$ phase becomes difficult to compress in the [100] direction as pressure increases. In addition, C_{44} slowly increases as the pressure increases. As we know, C_{44} is related to shear deformation resistance. The results show that the influence of the increase in external pressure on the shear deformation resistance is very limited.

The elastic modulus of the polycrystals can be obtained from the results of the single crystals by using the Voigt-Reuss-Hill (VRH) approximation[22]. For $Mg_3Zn_3Y_2$ phase with cubic crystal structures, the bulk modulus B and shear modulus G can be obtained by the following equations[23].

$$B=\frac{1}{3}\left(C_{11}+2C_{12}\right) \tag{3}$$

$$G=\frac{1}{5}\left(3C_{44}+C_{11}-C_{12}\right) \tag{4}$$

Further, Young's modulus E, Poisson's ratio v and elastic anisotropy coefficient A can be obtained by the following equations[20-24]:

$$E=\frac{9BG}{3B+G} \tag{5}$$

$$v=\frac{1}{2}\left[\frac{B-(2/3)G}{B+(1/3)G}\right] \tag{6}$$

$$A=\frac{2C_{44}}{C_{11}-C_{12}} \tag{7}$$

Table 3 shows the calculation results of the elastic modulus and Poisson's ratio of $Mg_3Zn_3Y_2$ at zero pressure. As can be seen, the results similar to other literatures[7], indicate that the current calculation method is reliable.

The calculated modulus (B, G, E) as a function of pressure are displayed in Fig.4. The bulk modulus B is used to represent the ability of the material to resist deformation under external pressure. Similarly, the shear modulus G can be used to measure the degree of material's resistance to deformation under shear stress. The Young's modulus E can be used as a measure of stiffness of the solid. It can be seen that the values of B, G and E increase with the pressure increasing. The results show that the W-$Mg_3Zn_3Y_2$ phase becomes hard to be compressed under high pressure. This indicates that the directional bonds among the Mg, Zn and Y atoms become stronger as the pressure increases. Thus, the external pressure enhances the mechanical properties of the W-$Mg_3Zn_3Y_2$ phase. It can also be seen that as the pressure increases, the bulk modulus B and Young's modulus E increase rapidly, whereas the shear modulus G increases slowly. It is indicated that the increasing of pressure has little effect on the shear modulus G, which is in good agreement with the analysis of the effect of pressure on the elastic constant C_{44}.

Fig.5 depicts the ratio of bulk modulus to shear modulus (B/G), Poisson's ratio v and the anisotropy index A as a function of pressure. Additionally, the ratio of bulk modules to shear modules (B/G) proposed by Pugh is used to predicate the ductility and brittleness of material[25]. If the B/G ratio is greater than 1.75, then the material behaves ductile, otherwise the material behaves brittle. The value of B/G ratio of $Mg_3Zn_3Y_2$ is 1.57 under zero pressure, implying that it is a brittle material. This is also consistent with the experimental result[26]. Additionally, it can be seen that B/G values increase with pressure, always above 1.75, indicating that $Mg_3Zn_3Y_2$ can have better ductility under higher pressures.

In addition, Cauchy pressure C_{12}–C_{44} can also be used to determine the ductility or brittleness of the material[27]. If the C_{12}–C_{44}<0, the material is brittle, whereas the material is

Table 2 Calculated elastic constants C_{ij} of $Mg_3Zn_3Y_2$ at zero pressure

C_{ij}	C_{11}	C_{12}	C_{44}
Present	75.5	44.4	47.8
Cal.[7]	86.2	42.9	48.7

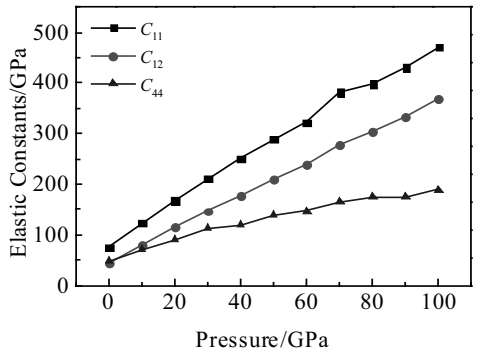

Fig.3 Calculated elastic constant C_{ij} of $Mg_3Zn_3Y_2$ as a function of pressure

Table 3 Calculated modulus, B/G, Poisson's ratio v and elastic anisotropy coefficient A of $Mg_3Zn_3Y_2$ at 0 GPa

Parameter	B/GPa	G/GPa	E/GPa	B/G	v	A	C_{12}–C_{44}
Present	54.8	34.9	86.3	1.57	0.24	3.07	–3.4
Cal. [7]	57.3	35.4	88.1	1.61	0.24	1.63	–5.8

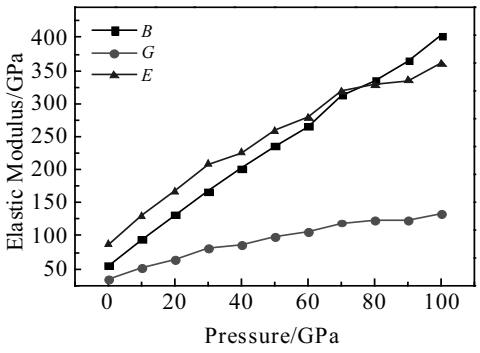

Fig.4 Variation trend of the calculated modulus (*B*, *G* and *E*) under different pressures

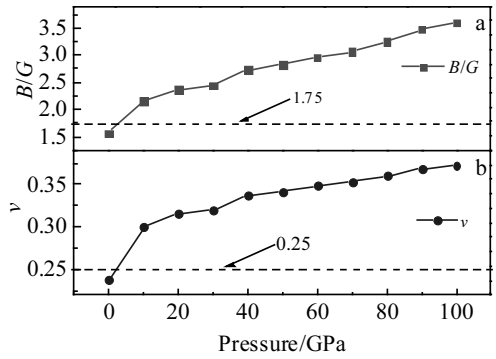

Fig.5 Calculated *B*/*G* (a) and Poisson's ratio *v* (b) of $Mg_3Zn_3Y_2$ as a function of pressure

ductile. Cauchy pressures as a function of external pressures of $Mg_3Zn_3Y_2$ compound are shown in Fig.6. As can be seen from Table 3 and Fig.6 that the C_{12}–C_{44} values of $Mg_3Zn_3Y_2$ at 0 GPa is negative, implying that it behaves brittle[28]. As can be seen from Fig.6, as the pressure increases, the value of C_{12}–C_{44} changes from a negative value to positive values, suggesting that $Mg_3Zn_3Y_2$ compound behave ductile under high pressure. This is exactly the same as the *B*/*G* results, indicating that the current calculations are correct.

The Poisson's ratio (*v*) is a measure of the crystal resistance against shear deformation, which is usually –1~0.5[29]. A large Poisson ratio indicates that the material has better plasticity[29,30]. It can be observed that the Poisson's ratio of $Mg_3Zn_3Y_2$ increases accordingly with the increase of pressure, indicating that $Mg_3Zn_3Y_2$ has a better plasticity. For a central boned force solid the Poisson's ratio *v* will have a value ranging from 0.25 to 0.5. The calculated Poisson's ratio of 0 GPa is very close to 0.25 and as pressure increases the Poisson's ratio is more than 0.25, meaning that the $Mg_3Zn_3Y_2$ crystal is boned with predominantly central interatomic forces. In addition, a large Poisson's ratio (*v*>0.25) will correspond to high anisotropy, which means that $Mg_3Zn_3Y_2$ compound would have

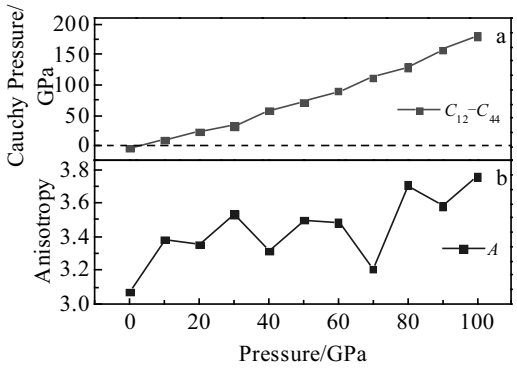

Fig.6 Calculated Cauchy pressure (a) and elastic anisotropy (b) of $Mg_3Zn_3Y_2$ as a function of pressure

higher anisotropy[31].

The anisotropy index (*A*) is an indicator of the degree of anisotropy in the solid structure[32]. As can be seen from Fig.6, since all *A* values are greater than 1, it is shown that $Mg_3Zn_3Y_2$ compounds exhibit anisotropy as the external pressure increases.

2.3 Melting temperature and hardness

It is well known that the properties of a material are closely associated with the melting temperature and hardness. The melting temperature and hardness are important indicators to evaluate the heat resistance and abrasive resistance of materials[33]. So it is necessary to investigate the melting temperature and hardness of $Mg_3Zn_3Y_2$ under pressure. In cubic intermetallic compounds, the melting temperature T_m can be estimated by using the elastic constant C_{11} [34], and the hardness *H* can be calculated according to the semi-empirical equation as follows[35]:

$$T_m = 553 + 5.91C_{11} \pm 300 \quad \text{(K)} \tag{8}$$

$$H = \frac{(1-2\nu)E}{6(1+\nu)} \tag{9}$$

The calculated T_m and *H* results are depicted in Fig.7. It can

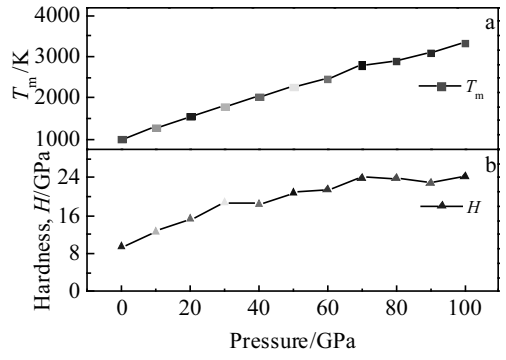

Fig.7 Melting points (a) and hardness (b) of $Mg_3Zn_3Y_2$ alloy under pressure

be seen that T_m increases as the pressure increases. Therefore, pressure can be applied to increase the heat resistance of $Mg_3Zn_3Y_2$. It can also be seen that the values of H increases with increasing pressure, and H has two stages under pressures: steadily increase with increasing pressure until reaching 30 GPa in the first stage and decreasing sharply when pressure exceeds 80 GPa at the second stage.

2.4 Electronic properties

In this work, the electronic density of state (DOS) is used to better understand the bonding characteristics of $Mg_3Zn_3Y_2$ phase and then to reveal the fundamental structural stability mechanism under high pressure. The total density of states (TDOS) and the partial density of states (PDOS) of $Mg_3Zn_3Y_2$ at zero pressure are depicted in Fig.8. It is found that there is no energy gap above the Fermi level, indicating that $Mg_3Zn_3Y_2$ exhibits a metallic character[36]. As shown in Fig.8, the main bonding peaks of $Mg_3Zn_3Y_2$ are located in the range from −8 eV to 0 eV, predominantly derived from Mg s, Mg p, Zn s, Zn p, Zn d and Y s Y p Y d orbits. There is a very sharp bonding peak between −7.69 and −6.28 eV, which is predominantly from the Zn 4d orbits, while the antibonding peaks between the Fermi level and 3.0 eV originate from the contribution of valance electron numbers from Mg 2s and 2p orbits with Zn 3p and Y 4d orbits.

In order to investigate the structural phase transition with pressure change, the total DOS of $Mg_3Zn_3Y_2$ under different pressures are calculated, as shown in Fig.9. It can be known from Fig.9 that there is no phase transition in $Mg_3Zn_3Y_2$ under high pressure. In addition, the TDOS curves and their variation trends are similar to the calculated results at 0 GPa. From Fig.9, it can be seen clearly that the TDOS curves gradually decline as the pressure increases due to the variation of the interaction potentials [37]. It also can be seen that the pseudo-gap in the vicinity of the Fermi level is broadened, indicating the high pressure makes the covalent bond stronger[38]. Further analysis found that the range of the valence band was enlarged. This shows that the delocalization of $Mg_3Zn_3Y_2$ phase is enhanced under high pressure.

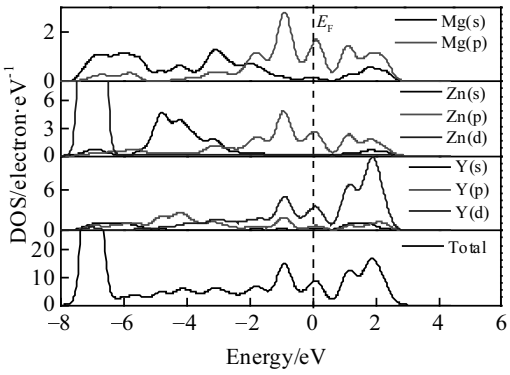

Fig.8 Density of states of $Mg_3Zn_3Y_2$ alloy under zero pressure

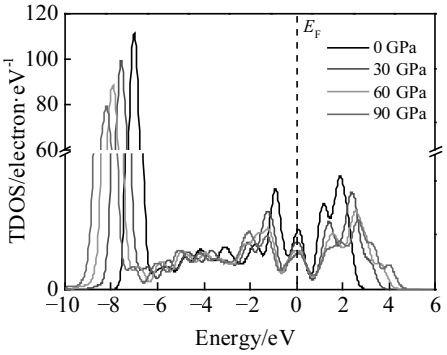

Fig.9 Total density of states of $Mg_3Zn_3Y_2$ alloy under different pressures

3 Conclusions

1) The lattice parameter a and the volume V of $Mg_3Zn_3Y_2$ decrease with increasing the external pressure, while the structural stability decreases with increasing external pressure.

2) The elastic constants and the polycrystalline elastic parameters (B, G, E and v) increase with increasing the external pressure.

3) The B/G values and Cauchy pressure indicate that $Mg_3Zn_3Y_2$ compound behaves brittle at 0 GPa and the pressure can enhance the ductility.

4) The melting temperature and hardness increase with the increasing the pressure.

5) The calculation result of density of state (DOS) under high pressure reveals that there is no phase transition with pressure changing.

References

1 Chen Y, Wang Y, Gao J J. *Journal of Alloys and Compounds*[J], 2018, 740: 727

2 Němec M, Jäger A, Tesařc K *et al*. *Materials Characterization*[J], 2017, 134: 69

3 Yu J Y, Wang J Z, Li Q *et al*. *Rare Metal Materials and Engineering*[J], 2016, 45(11): 2757

4 Wu M M, Jiang Y, Wang J W *et al*. *Journal of Alloys and Compounds*[J], 2011, 509(6): 2885

5 Gao Y, Chen W L, Guo Z. *Rare Metal Materials and Engineering*[J], 2017, 46(8): 2070

6 Antion C, Donnadieu P, Perrard F *et al*. *Acta Materialia*[J], 2003, 51(18): 5335

7 Tang B Y, Wang N, Yu W Y *et al*. *Acta Materialia*[J], 2008, 56(14): 3353

8 Gröbner J, Kozlov A, Fang X Y *et al*. *Acta Materialia*[J], 2015, 90: 400

9 Ma Z N, Jiang M, Wang L. *Acta Physica Sinica*[J], 2015, 64(18): 187 102

10 Ma Z N, Wang X, Yan T T *et al*. *Journal of Alloys and*

Compounds[J], 2017, 708: 29
11 Mao P L, Yu B, Liu Z *et al*. *Computational Materials Science*[J], 2014, 88: 61
12 Peivaste I, Alahyarizadeh G, Minuchehr A *et al*. *Vacuum*[J], 2018, 154: 37
13 Guo Y L, Chen J C, Wang C Y *et al*. *Journal of Nuclear Materials*[J], 2018, 508: 147
14 Payne M C, Teter M P, Allan D C *et al*. *Reviews of Modern Physics*[J], 1992, 64(4): 1045
15 Wang F, Sun S J, Yu B *et al*. *Transactions of Nonferrous Metals Society of China*[J], 2016, 26(1): 203
16 Perdew J P, Burme K, Ernzerhof M. *Physical Review Letters*[J], 1996, 77: 3865
17 Ma S Y, Liu L M, Wang S Q. *Journal of Materials Science*[J], 2013, 48(4): 1407
18 Zhang H, Shang S L, Wang Y *et al*. *Acta Materialia*[J], 2010, 58(11): 4012
19 Niu X F, Huang Z W, Wang H *et al*. *Rare Metal Materials and Engineering*[J], 2018, 47(5): 1325
20 Zhao C Y, Wang X Y. *Journal of Alloys and Compounds*[J], 2017, 704: 484
21 Tian J Z, Zhao Y H, Wen Z Q *et al*. *Solid State Communications* [J], 2017, 257: 6
22 Liu Y Z, Xing J D, Fu H G *et al*. *Physics Letters A*[J], 2017, 381(32): 2648
23 Sari A, Merad G, Abdelkader H S. *Computational Materials Science*[J], 2015, 96: 348
24 Ghebouli B, Ghebouli M A, Fatmi M *et al*. *Solid State Communications*[J], 2010, 150(39-40): 1896
25 Chen Z, Zhang P, Chen D *et al*. *Journal of Applied Physics*[J], 2015, 117(8): 1909
26 Xu D K, Tang W N, Liu L *et al*. *Journal of Alloys and Compounds*[J], 2007, 432(1-2): 129
27 Mian S A, Muzammil M, Rahman G *et al*. *Mater Sci-Poland*[J], 2017, 35(1): 197
28 Korozlu N, Colakoglu K, Deligoz E *et al*. *Journal of Alloys and Compounds*[J], 2013, 546: 157
29 Li C, Zhang K, Ru J G. *Journal of Alloys and Compounds*[J], 2015, 647: 573
30 Hu W C, Liu Y, Li D J *et al*. *Computational Materials Science*[J], 2014, 83: 27
31 Li Y L, Zeng Z. *Solid State Communications*[J], 2009, 149: 1591
32 Mcnamara A K, Keken P E V, Karato S I. *Nature*[J], 2002, 416(6878): 310
33 Mao P L, Yu B, Liu Z *et al*. *Journal of Applied Physics*[J], 2015, 117(11): 115 903
34 Fine M E, Brown L D, Marcus H L. *Scripta Materialia*[J], 1984, 18(9): 951
35 Yousef E S, Ei-adawy A, Ei-kheshkhany N. *Solid State Communications*[J], 2006, 139(3): 108
36 Birsan A. *Current Applied Physics*[J], 2014, 14(11): 1434
37 Liu Y, Hu W C, Li D J *et al*. *Intermetallics*[J], 2012, 31: 257
38 Mao P L, Yu B, Liu Z *et al*. *Computational Materials Science*[J], 2014, 88(1): 61

压力对 $Mg_3Zn_3Y_2$ 相的结构、物理和电子性能影响的第一性原理计算

高　岩[1,2]，毛萍莉[1]，刘　正[1]，王　峰[1]，王　志[1]
(1. 沈阳工业大学，辽宁 沈阳 110870)
(2. 沈阳师范大学，辽宁 沈阳 110034)

摘　要：利用基于密度泛函理论（DFT）的第一性原理计算方法，研究了压力对面心立方化合物 $Mg_3Zn_3Y_2$ 的结构、弹性和电子性能的影响。计算并分析了 $Mg_3Zn_3Y_2$ 的弹性常数。基于弹性常数的计算结果，推导了 $Mg_3Zn_3Y_2$ 的体积模量（B），剪切模量（G），杨氏模量（E），泊松比（ν），各向异性指数（A），熔点和硬度。结果表明，在 0 GPa 下优化的晶格常数与其他计算和实验结果相吻合，压力的增加可以促进 $Mg_3Zn_3Y_2$ 物理性能的提高。此外，$Mg_3Zn_3Y_2$ 的各向异性指数（A）随压力的增加而增加。通过对电子态密度的分析表明，随着压力的增加，$Mg_3Zn_3Y_2$ 相的结构稳定性降低。

关键词：第一性原理计算；镁合金；弹性性能；电子结构

作者简介：高　岩，男，1983 年生，博士，沈阳工业大学材料科学与工程学院，辽宁 沈阳 110870，电话：024-86593280，E-mail: gaoy@synu.edu.cn